NACA RM A54H26b

RESEARCH MEMORANDUM

WIND-TUNNEL INVESTIGATION AT SUBSONIC AND SUPERSONIC SPEEDS OF A FIGHTER MODEL EMPLOYING A LOW-ASPECT-RATIO UNSWEPT WING AND A HORIZONTAIL TAIL MOUNTED WELL ABOVE THE WING PLANE- LATERAL AND DIRECTIONAL STABILITY

By Benton E. Wetzel

Ames Aeronautical Laboratory
Moffett Field, Calif.

NATIONAL ADVISORY COMMITTEE
FOR AERONAUTICS

WASHINGTON
April 28, 1955

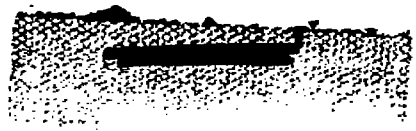

NATIONAL ADVISORY COMMITTEE FOR AERONAUTICS

RESEARCH MEMORANDUM

WIND-TUNNEL INVESTIGATION AT SUBSONIC AND SUPERSONIC SPEEDS OF A FIGHTER MODEL EMPLOYING A LOW-ASPECT-RATIO UNSWEPT WING AND A HORIZONTAL TAIL MOUNTED WELL ABOVE THE WING PLANE - LATERAL AND DIRECTIONAL STABILITY[1]

By Benton E. Wetzel

SUMMARY

The static lateral- and directional-stability characteristics of a high-speed fighter-type airplane, obtained from wind-tunnel tests of a model, are presented. The model consisted of a thin, unswept wing of aspect ratio 2.5 and taper ratio 0.385, a body, and a horizontal tail mounted in a high position on a vertical tail. Rolling-moment, yawing-moment, and cross-wind-force coefficients are presented for a range of sideslip angles of -5° to $+5^\circ$, for Mach numbers of 0.90, 1.45, and 1.90.

Data are presented which show the effects on the lateral and directional stability of: (1) component parts of the complete model, (2) modification of the empennage so as to provide different heights of the horizontal tail above the wing plane, (3) angle of attack, and (4) dihedral of the wing.

INTRODUCTION

A model of a high-speed fighter airplane has been the subject of an investigation at subsonic and supersonic speeds in the Ames 6- by 6-foot supersonic wind tunnel. The model is representative of current designs for airplanes with unswept-wing plan forms and with horizontal tails mounted well above the wing-chord plane. In order to determine which design arrangements offer promise from the standpoint of static longitudinal and directional stability, various combinations of the model components have been tested. The results of these tests provide information regarding the effect of mutual interference on the contributions of the components to the stability of the complete model.

[1]The information presented herein was originally made available to the U. S. military air services in a report dated August 26, 1954.

This report presents the results of the lateral and directional investigation of that model, and is a companion paper to an earlier research memorandum (ref. 1) which was concerned with the longitudinal-stability characteristics of the model. The primary purposes of this paper are to point out some of the important interference effects, especially those between the horizontal- and vertical-tail surfaces, and to show their contributions to the static lateral and directional stability.

NOTATION

All force coefficients presented herein are referred to the wind axes; all moment coefficients to the stability axes. The moment center was placed at the projection of the 25-percent mean aerodynamic chord point on the longitudinal axis of the body.

The following notation has been used in this report:

b model wing span, in.

C_l rolling-moment coefficient, $\frac{\text{rolling moment}}{qSb}$

C_n yawing-moment coefficient, $\frac{\text{yawing moment}}{qSb}$

C_Y cross-wind-force coefficient, $\frac{\text{cross-wind force}}{qS}$

c local chord of the wing, in.

$\bar{c}$ mean aerodynamic chord of the wing, $\frac{\int_0^{b/2} c^2 dy}{\int_0^{b/2} c\, dy}$, in.

h height of the horizontal tail above the body axis, in.

l_t horizontal-tail length, measured between the 25-percent mean aerodynamic chord stations of the wing and the horizontal tail, in.

l_v vertical-tail length, measured between the 25-percent mean aerodynamic chord stations of the wing and the vertical tail, in.

M free-stream Mach number

q free-stream dynamic pressure, lb/sq in.

R Reynolds number, based on the mean aerodynamic chord

[redacted]

S model wing area, formed by extending the leading and trailing edges to the plane of symmetry, sq in.

S_V area of vertical tail, including portion enclosed in body by extending leading edge to body axis, sq in.

y spanwise distance from plane of symmetry, in.

α angle of attack of the body, deg

β angle of sideslip, deg

Γ angle of wing dihedral, deg

In addition, the following notation has been used in order to denote various components of the model:

B body

H_1 horizontal tail, when located 7.13 inches above the body axis

H_2 horizontal tail, when located 8.15 inches above the body axis

V_1 vertical tail used with horizontal tail H_1

V_2 vertical tail used with horizontal tail H_2

W wing

APPARATUS AND MODEL

The experimental investigation was performed in the Ames 6- by 6-foot supersonic wind tunnel. This wind tunnel, which has a closed section and is of the variable-pressure type, is operated at Mach numbers varying from 0.60 to 0.90 and from 1.20 to 1.90. A complete description of the wind tunnel and the characteristics of the air stream at supersonic speeds can be found in reference 2. In this wind tunnel, models are sting-mounted and the forces on the models are measured with internal electrical strain-gage balances. The balance used for the present tests was of the flexure-pivot type. A photograph of the model mounted in the wind tunnel is shown in figure 1.

The complete model consisted of an unswept wing of aspect ratio 2.5, a horizontal tail mounted in a high position on a vertical tail, and a body with a circular cross section modified by the addition of a canopy and protuberances simulating side inlets. A dimensional sketch of the

model and its parts is shown in figure 2, and a compilation of the geometric characteristics is presented in table I. The model was designed to permit tests of the wing and body as a unit and in combination with various components of the empennage. Two different vertical tails were built, which allowed mounting the horizontal tail in two different positions above the plane of the wing. All parts of the model were made of steel, with the exception of the body, which was constructed of aluminum.

TESTS AND PROCEDURES

Range of Test Variables

Rolling moment, yawing moment, and cross-wind force were measured throughout a range of sideslip angles varying from -5° to $+5^\circ$ at Mach numbers of 0.90, 1.45, and 1.90, at a Reynolds number of 2.4 million. Although most of the tests were performed at zero angle of attack, some data were obtained at an angle of attack of 5°. Tests were made of a number of combinations of the components of the model. The various combinations and test conditions are enumerated in table II.

Reduction of Data

Data presented herein have been reduced to NACA coefficient form. The reader is referred to the section on notation for complete descriptions of the coefficients used. It should be noted that the cross-wind-force coefficient is referred to the wind axes, while the rolling- and yawing-moment coefficients are referred to the stability axes.

Corrections have been made to the data to account for differences known to exist between measurements made in the wind tunnel and in a free-air stream. Corrections made to the data presented herein account for the following factors:

1. The increase in airspeed in the vicinity of the model at subsonic speed as a result of constriction of the air stream by the walls of the wind tunnel.

2. The change in angle of attack of the model induced by the walls of the wind tunnel at subsonic speeds as a consequence of the lift on the model. The correction amounted to: $\Delta\alpha = 0.315\ C_L$.

It should be pointed out that, for the lateral tests, the model was mounted in the wind tunnel with the wing horizontal. As a result, nonuniformities of the air stream had a greater effect on the data presented in this report than on those of reference 1. The reader's attention is

[redacted]

directed to reference 2, wherein he will find detailed information about the characteristics of the air stream at supersonic speeds.

RESULTS AND DISCUSSION

Results are presented herein which show the effects of the following on the lateral and directional stability:

1. Various components of the complete model
2. Modification of the empennage so as to provide different heights of the horizontal tail above the wing plane
3. Angle of attack
4. Dihedral of the wing

Although all of these results will be discussed, the primary purpose of this report is to discuss some of the important effects of interference between component parts on the lateral- and directional-stability characteristics of the complete model. The interferences discussed are some of those which affect the contributions of the tail surfaces to the stability and not those which affect the contributions of the wing and body. Although the tests performed did not allow a complete quantitative separation of these interference effects, they did provide an instructive qualitative study.

Effects of Model Components

The effects of various components of the model on the variation with sideslip angle of the rolling-moment, yawing-moment, and cross-wind-force coefficients are shown in figure 3. The wing-body combination was unstable both laterally and directionally. When the vertical tail was added to the wing-body model, the large cross-wind force carried by the vertical tail resulted in rolling- and yawing-moment contributions large enough to provide lateral and directional stability.

With the addition of the horizontal tail, the model was provided with additional lateral and directional stability, as a result of two effects arising from the mutual interference between the horizontal- and vertical-tail surfaces. Consider, first, the effect of the addition of the horizontal tail on the characteristics of the vertical tail. This, the so-called end-plate effect of the horizontal tail in increasing the effective aspect ratio of the vertical tail, resulted in an increased rate of change of cross-wind force with sideslip angle at a Mach number of 0.90. This effect increased both the lateral and the directional stability at that

Mach number. At supersonic speed, the influence of the horizontal tail decreased with increasing Mach number since the influence of the tail was confined within the Mach cone from the tip of the vertical tail.

The second interference effect, that of the vertical tail on the characteristics of the horizontal tail, occurred at both subsonic and supersonic speeds. Because the horizontal tail was located near the tip of the vertical tail, only its lower surface was influenced by the loading on the vertical tail. The pressure differential between the two surfaces of the vertical tail induced an asymmetric loading on the horizontal tail which resulted in additional lateral stability for the complete model.

Effect of Modifying Empennage

The effect on the lateral and directional stability of modifying the empennage so as to mount the horizontal tail in a higher position above the wing plane is shown in figure 4. The results showed that the model with the higher horizontal tail was more stable both laterally and directionally. Although a first appraisal of these data might indicate a significant effect of horizontal-tail height, analysis of the data indicated that most of the increased stability could be accounted for by the larger span and greater aspect ratio of the vertical tail used with the higher horizontal tail. Since the nondimensional tail height (the ratio of horizontal-tail height h to vertical-tail span) was not significantly different for the two empennages, no difference in the end-plate effect at subsonic speeds should be expected.

Effect of Angle of Attack

The effect of angle of attack on the lateral and directional stability of the wing-body and the wing-body-tail combinations is presented in figure 5. As in the case at zero angle of attack, the wing-body combination was unstable both laterally and directionally at an angle of attack of 5°. The lateral instability was, of course, decreased when the model was tested at $\alpha = 5^\circ$.

The lateral and directional stability of the complete model increased as angle of attack increased except at $M = 1.90$, where this effect was reversed. The increase in directional stability at $M = 0.90$ and $M = 1.45$ resulted from an increase in cross-wind force carried by the vertical tail, believed attributable to the sidewash component of the vorticity discharged from the wing. At $M = 1.90$, however, the vertical tail lies outside the Mach cones from the wing tips but within the region bounded by the waves from the leading and trailing edges of the wing. Since the vertical tail was no longer influenced by the vorticity from the wing

tips but was primarily influenced by the flow field above the wing, it is not surprising that the cross-wind force and the attendant rolling and yawing moments produced by the tail were reduced.

Effect of Dihedral

The effect of variation of wing dihedral is presented in figure 6 for the wing-body and wing-body-tail combinations. As would be expected, variation of dihedral affected primarily the lateral stability of the models. The variation of wing dihedral caused only small differences in the contributions of the tail surfaces to the lateral and directional stability of the complete model.

CONCLUDING REMARKS

Wind-tunnel studies of a model of a fighter airplane with an unswept wing showed that mutual interference between the vertical- and horizontal-tail surfaces played a significant role in the contribution of the empennage to the stability of the complete airplane. The horizontal tail, mounted near the tip of the vertical tail, acted as an end plate and increased the loading on the vertical tail, resulting in an increase in the contribution of the vertical tail to both the lateral and directional stability at a Mach number of 0.90. The presence of the vertical tail resulted in an asymmetric loading on the horizontal tail which provided a small amount of additional lateral stability at both subsonic and supersonic speeds.

Ames Aeronautical Laboratory
National Advisory Committee for Aeronautics
Moffett Field, Calif., Aug. 26, 1954.

[redacted]

REFERENCES

1. Smith, Willard G.: Wind-Tunnel Investigation at Subsonic and Supersonic Speeds of a Fighter Model Employing a Low-Aspect-Ratio Unswept Wing and a Horizontal Tail Mounted Well Above the Wing Plane - Longitudinal Stability and Control. NACA RM A54D05, 1954.

2. Frick, Charles W., and Olson, Robert N.: Flow Studies in the Asymmetric Adjustable Nozzle of the Ames 6- by 6-Foot Supersonic Wind Tunnel. NACA RM A9E24, 1949.

TABLE I.- GEOMETRIC CHARACTERISTICS OF THE MODEL

Wing	
Aspect ratio	2.50
Taper ratio	0.385
Airfoil section (streamwise)	Modified biconvex with elliptical leading edge
Thickness-chord ratio, percent chord	3.4
Area, S, sq in.	202.50
Chord at plane of symmetry, in.	13.00
Chord at tip, in.	5.00
Mean aerodynamic chord, in.	9.59
Span	22.50
Dihedral, deg	-5 or -10
Incidence, deg	0
Sweep of leading edge, deg	27.1
Body	
Length, in.	45.39
Vertical tail, V_1	
Stabilizer	
Aspect ratio	1.07
Airfoil section (parallel to body axis)	Modified biconvex with sharp leading edge
Thickness-chord ratio for section 2.32 in. above body axis, percent chord	4.25
Thickness-chord ratio for section 7.13 in. above body axis, percent chord	5.00
Area, S_V, including portion enclosed in body by extending leading edge to body axis, sq in.	59.51
Chord of airfoil section 2.32 in. above body axis, in.	9.65
Chord of airfoil section 7.13 in. above body axis, in.	4.46
Mean aerodynamic chord, in.	7.93
Span, in.	7.98
Tail length, l_V, in.	12.93
Tail volume, $\frac{l_V}{b}\frac{S_V}{S}$	0.1689
Sweep of leading edge, deg	44
Dorsal fin	
Area, exposed, sq in.	2.17
Total exposed area, stabilizer and dorsal fin, sq in.	44.64
Vertical tail, V_2	
Stabilizer	
Aspect ratio	1.26
Airfoil section (parallel to body axis)	Modified biconvex with elliptical leading edge
Thickness-chord ratio for section 2.32 in. above body axis, percent chord	4.5

[redacted]

TABLE I.- GEOMETRIC CHARACTERISTICS OF THE MODEL - Concluded

Thickness-chord ratio for section 8.15 in. above body axis, percent chord	5.25
Area, S_V, including portion enclosed in body by extending leading edge to body axis, sq in.	60.60
Chord of airfoil section 2.32 in. above body axis, in.	9.18
Chord of airfoil section 8.15 in. above body axis, in.	4.12
Mean aerodynamic chord, in.	7.35
Span, in.	8.75
Tail length, l_V, in.	13.24
Tail volume, $\frac{l_V}{b}\frac{S_V}{S}$	0.1761
Sweep of leading edge, deg	38
Dorsal fin	
Area, exposed, sq in.	2.38
Total exposed area, stabilizer and dorsal fin, sq in.	44.88
Horizontal tail (both H_1 and H_2)	
Aspect ratio	2.89
Taper ratio	0.326
Airfoil section (streamwise)	Modified biconvex with elliptical leading edge
Thickness-chord ratio at plane of symmetry, percent chord	5
Thickness-chord ratio at tip, percent chord	3
Area, sq in.	49.80
Chord at plane of symmetry, in.	6.26
Chord at tip, in.	2.04
Mean aerodynamic chord, in.	4.51
Span, in.	12.00
Tail length, l_t, in.	17.22
Dihedral, deg	0
Incidence, deg	0
Sweep of 50-percent-chord line, deg	0

TABLE II.- MODEL COMBINATIONS AND TEST CONDITIONS

Model	Γ, deg	α, deg	Figure no.
WB	-5	0	6
	-10	0	3, 5, 6
	-10	5	5
WBV_1	-10	0	3
WBV_1H_1	-10	0	3, 4, 5
	-10	5	5
WBV_2H_2	-5	0	6
	-10	0	4, 6

[redacted]

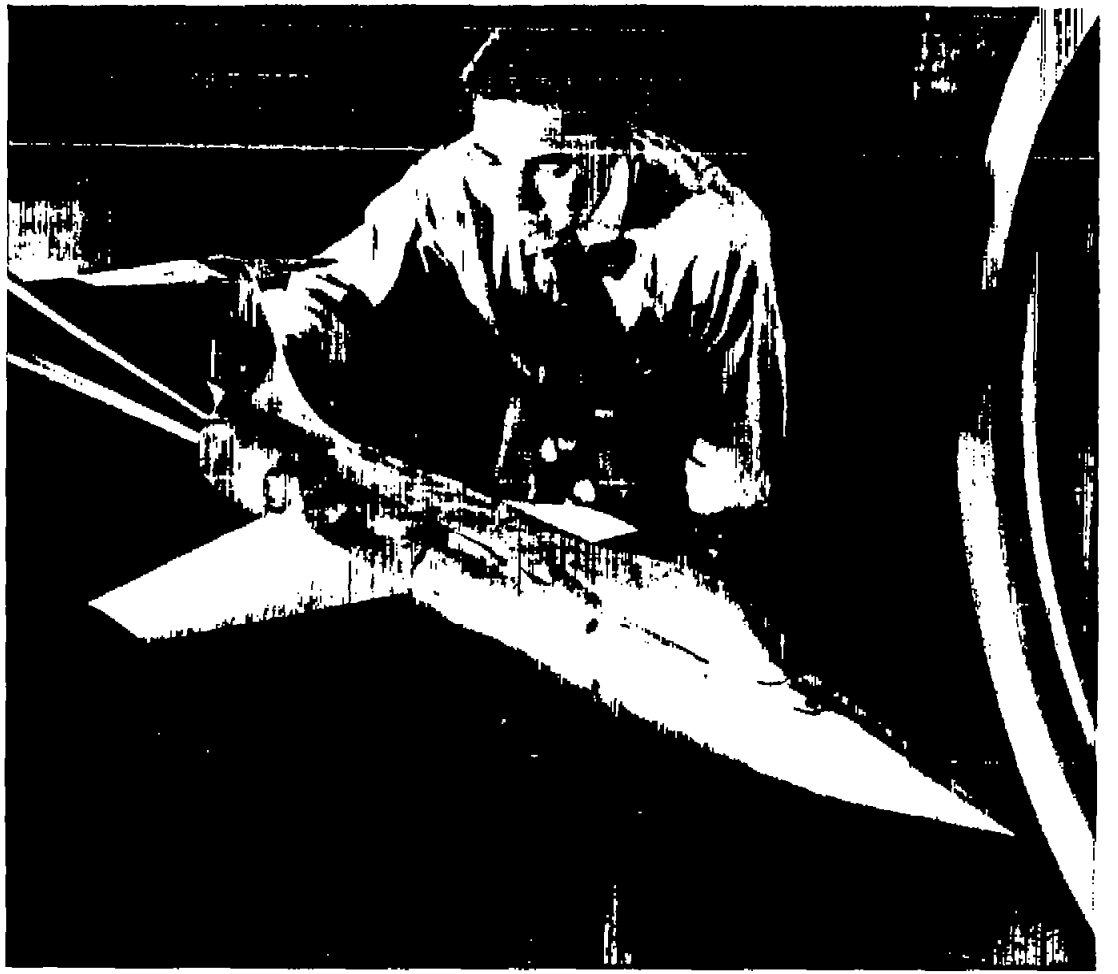

A-18101.1

Figure 1.- Three-quarter front view of fighter model in the Ames 6- by 6-foot supersonic wind tunnel.

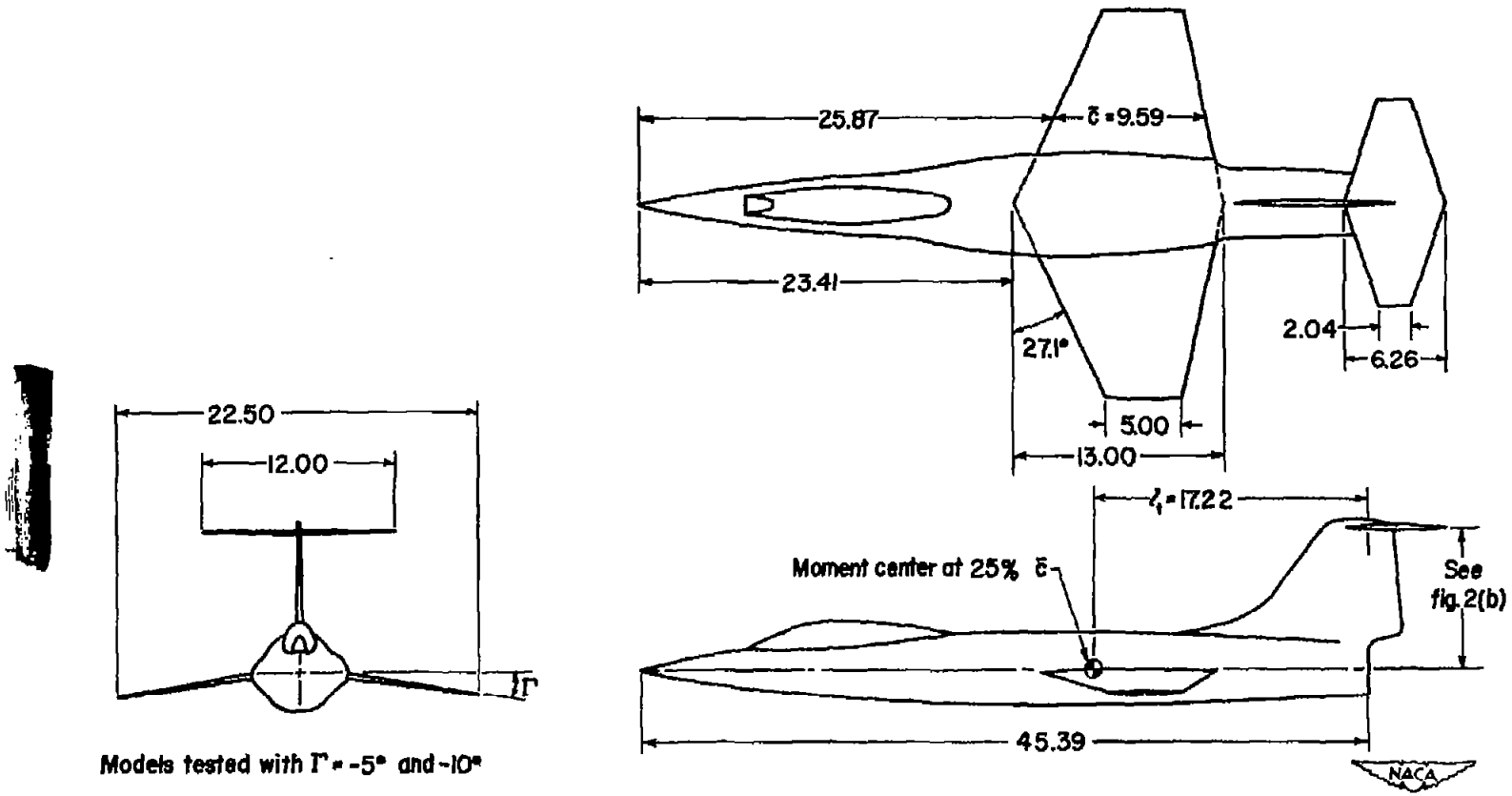

(a) Three-view sketch of model.

Figure 2.- Dimensional sketches of models.

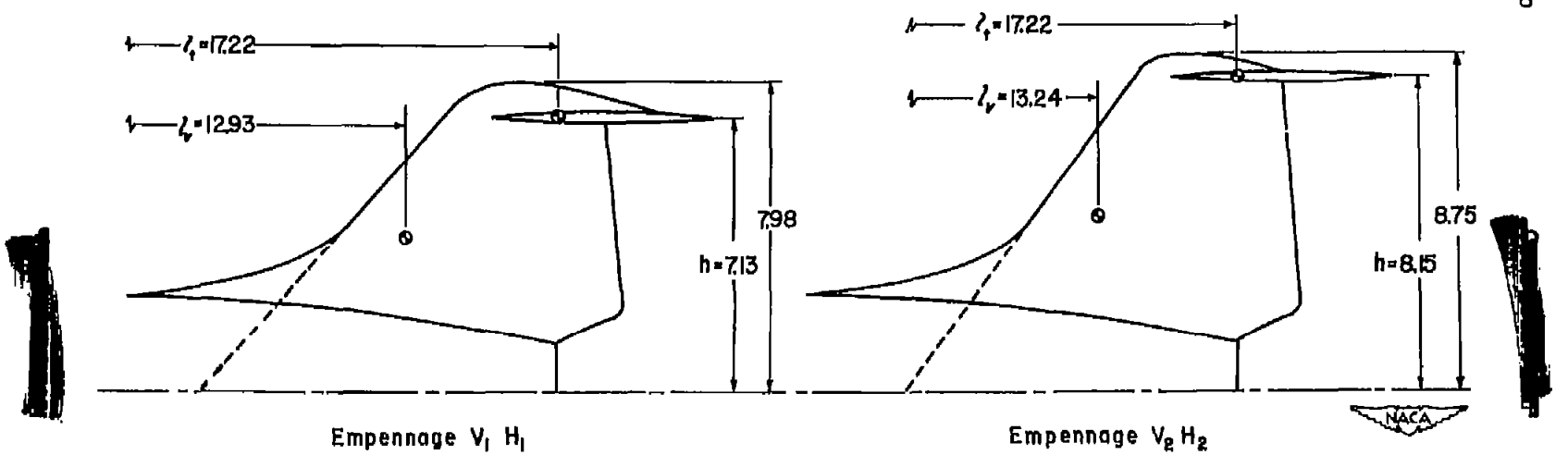

(b) Empennages tested.

Figure 2.- Concluded.

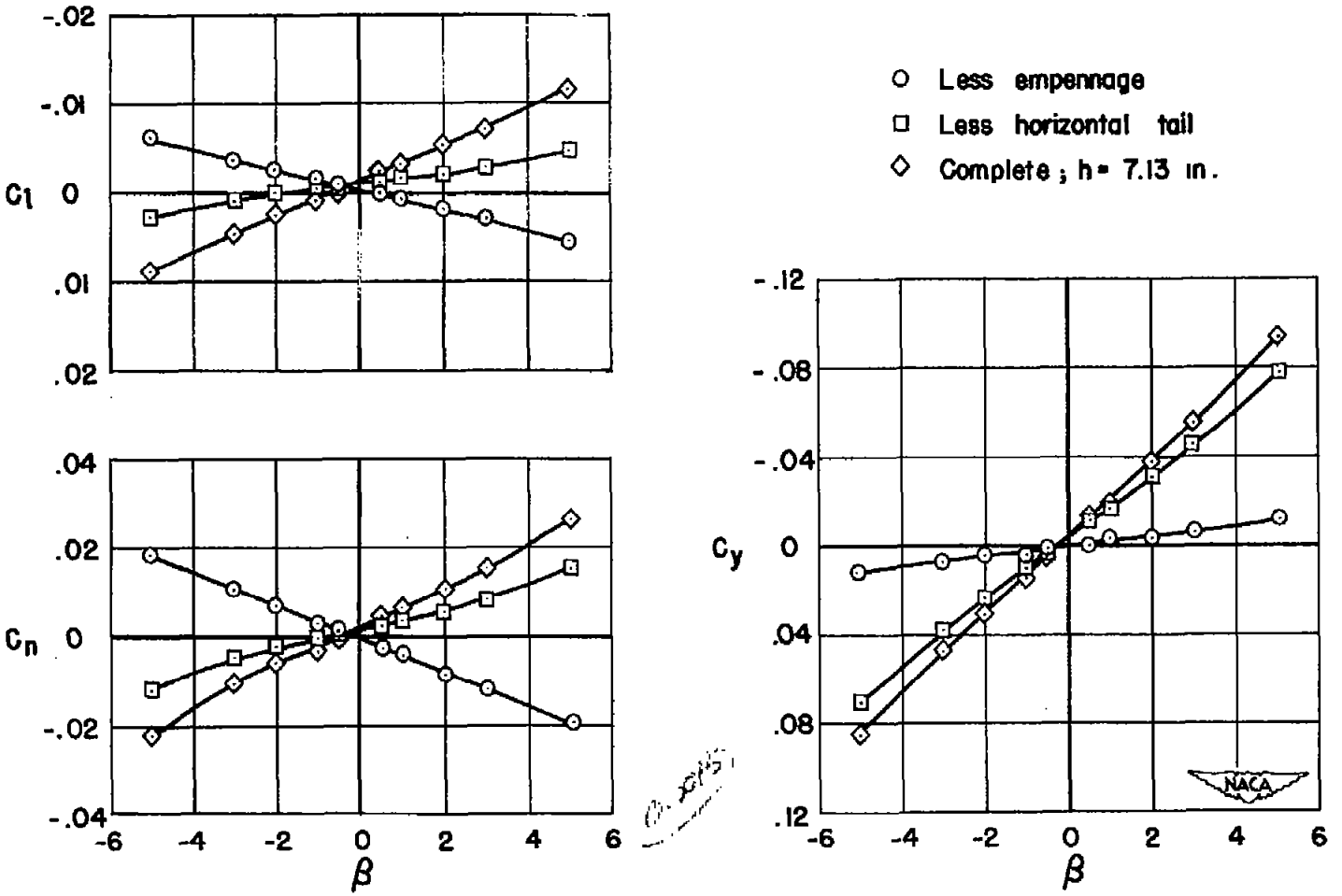

(a) M = 0.90

Figure 3.- Effect of model components on the variation with sideslip angle of the rolling-moment, yawing-moment, and cross-wind-force coefficients for a model of a fighter airplane; $\Gamma = -10^\circ$; $\alpha \approx 0^\circ$.

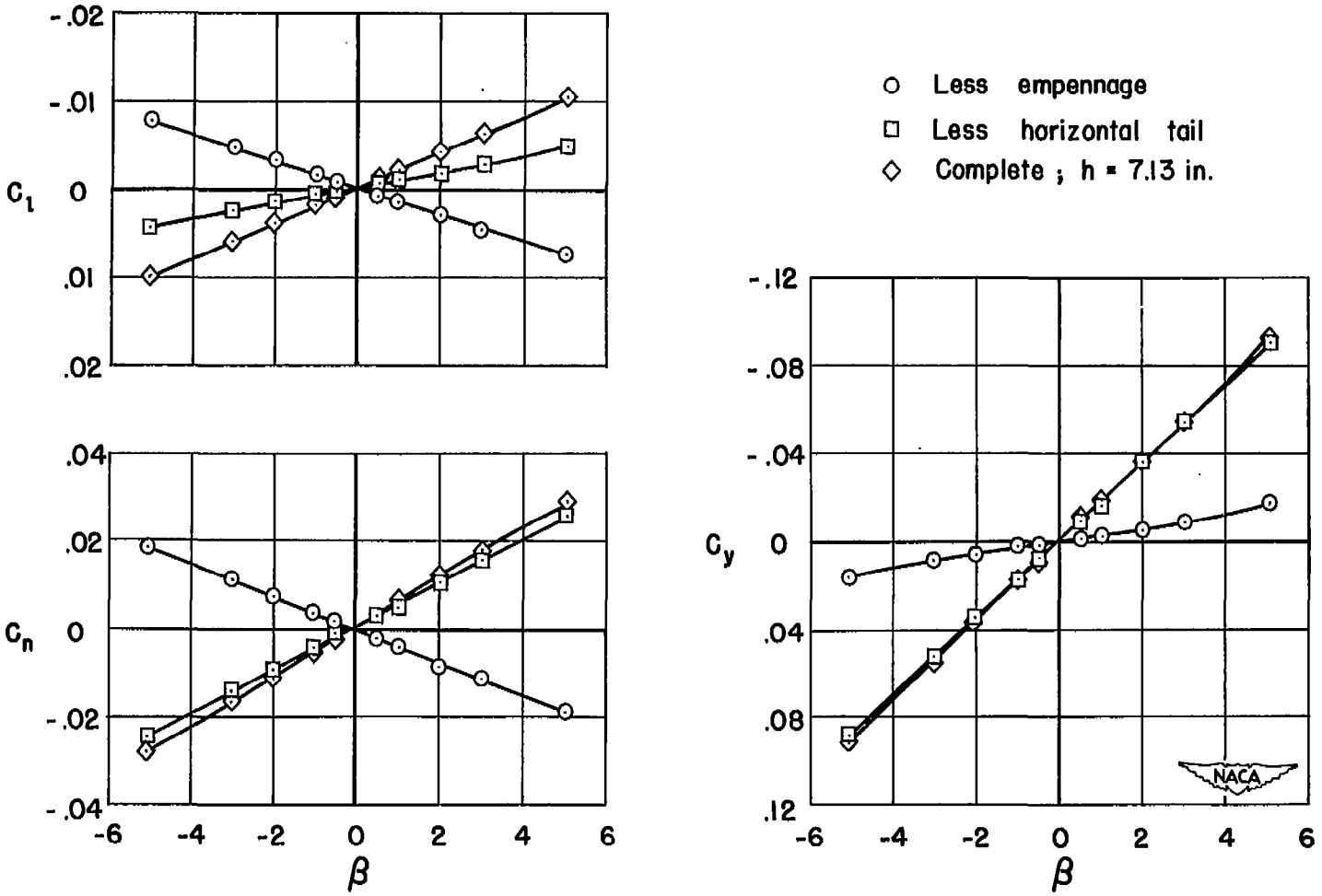

(b) M = 1.45

Figure 3.- Continued.

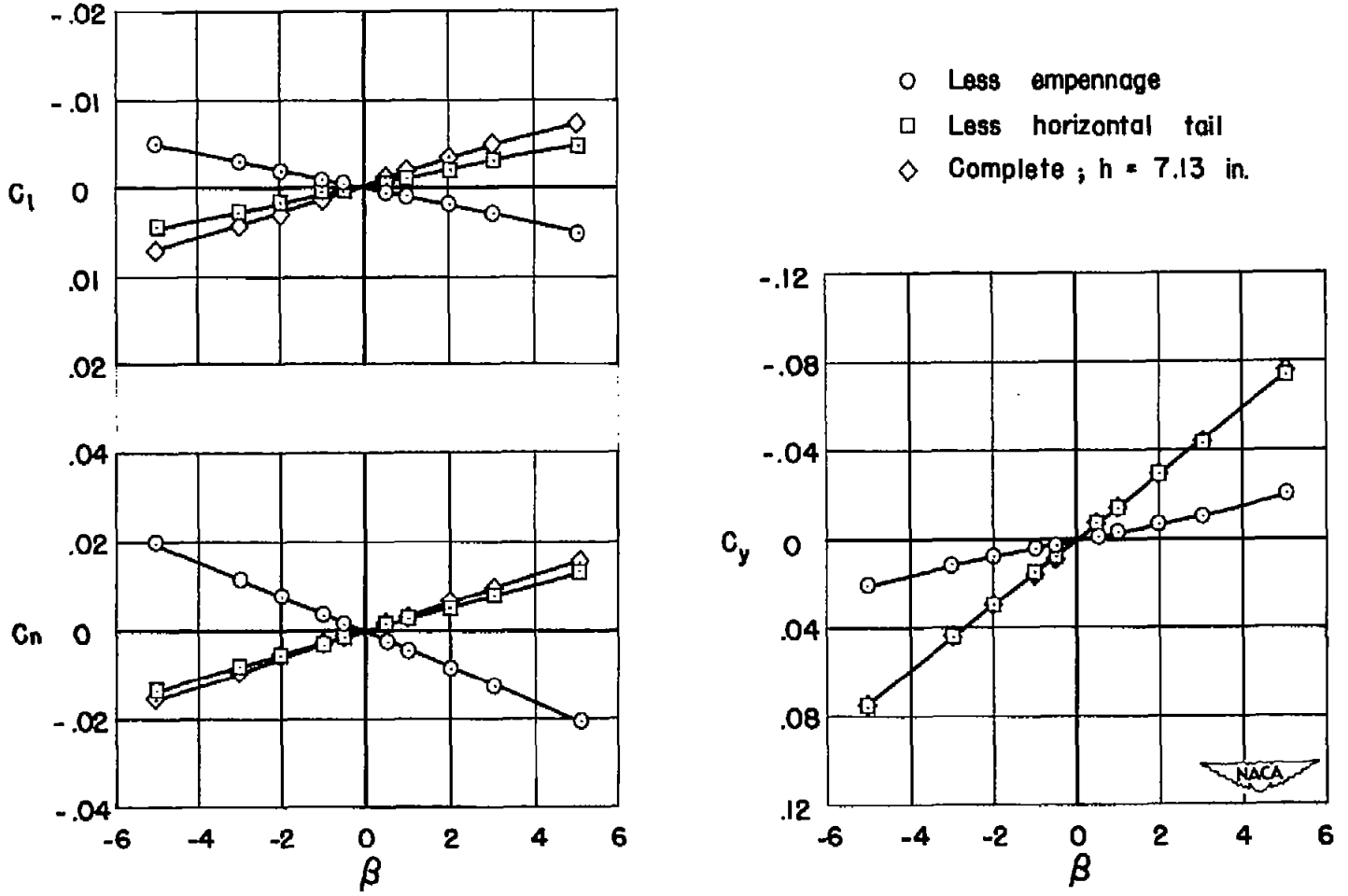

(c) M = 1.90

Figure 3.- Concluded.

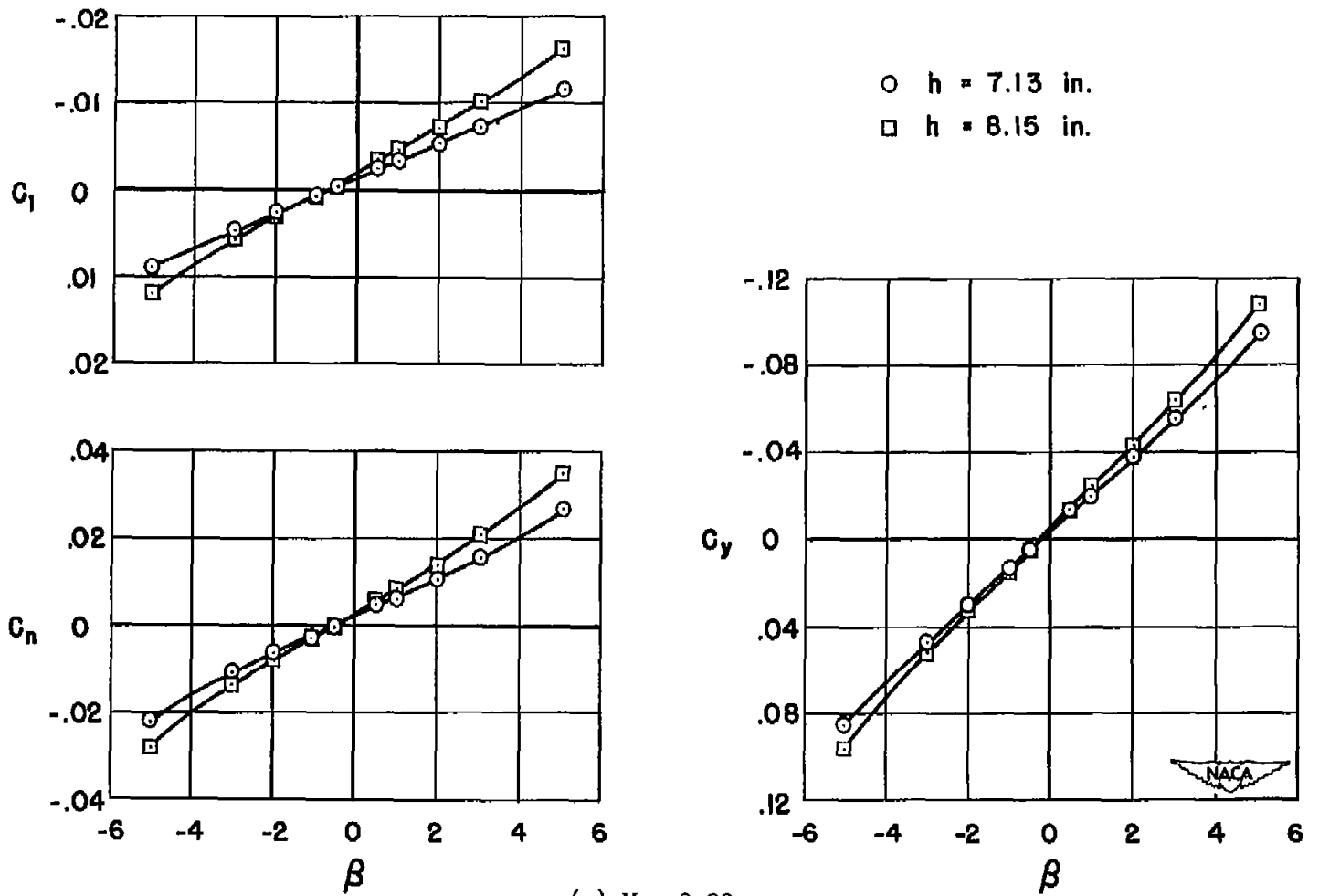

(a) M = 0.90

Figure 4.- Effect of modifying the empennage on the variation with sideslip angle of the rolling-moment, yawing moment, and cross-wind-force coefficients for a model of a fighter airplane; $\Gamma = -10^\circ$, $\alpha \approx 0^\circ$.

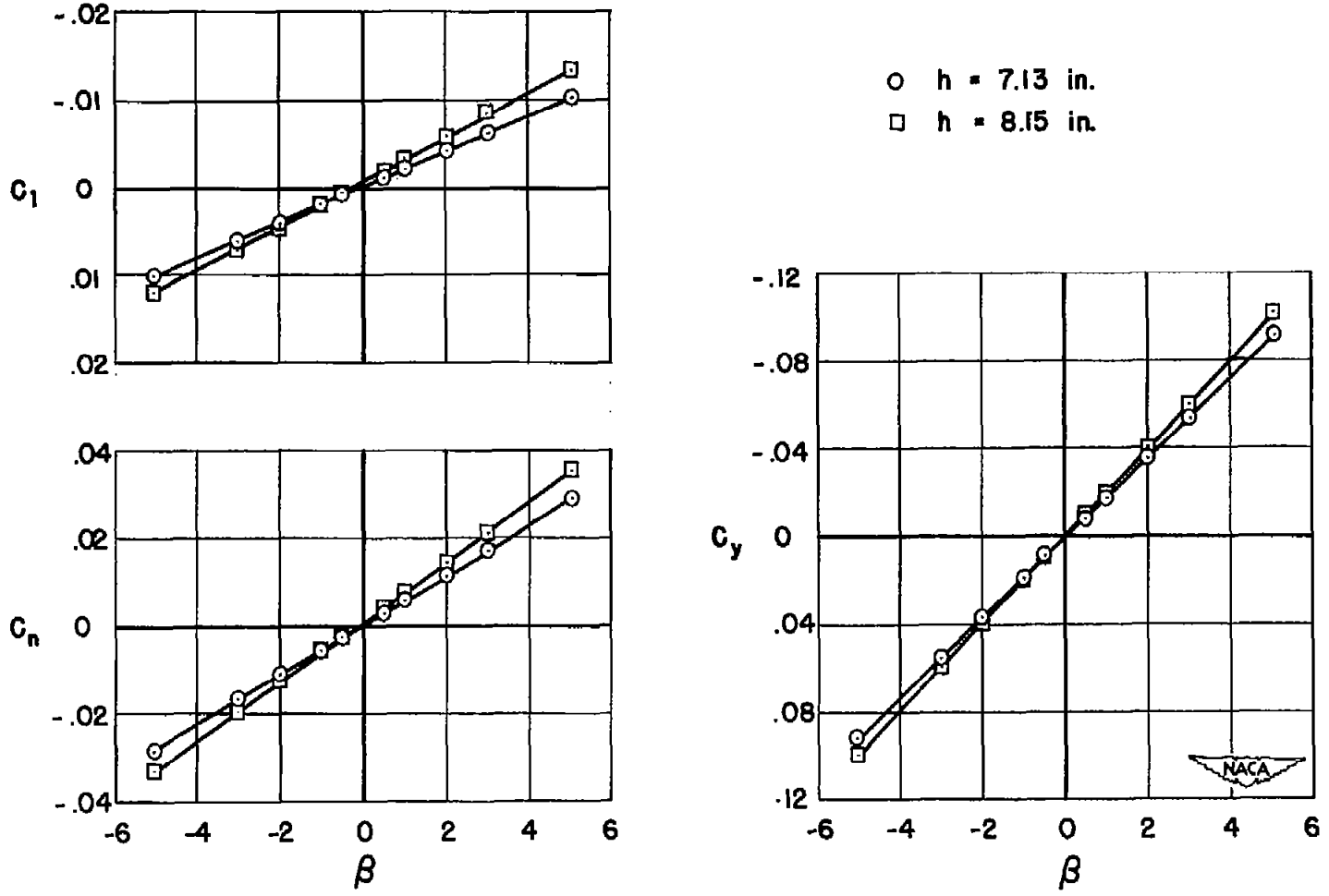

(b) M = 1.45

Figure 4.- Continued.

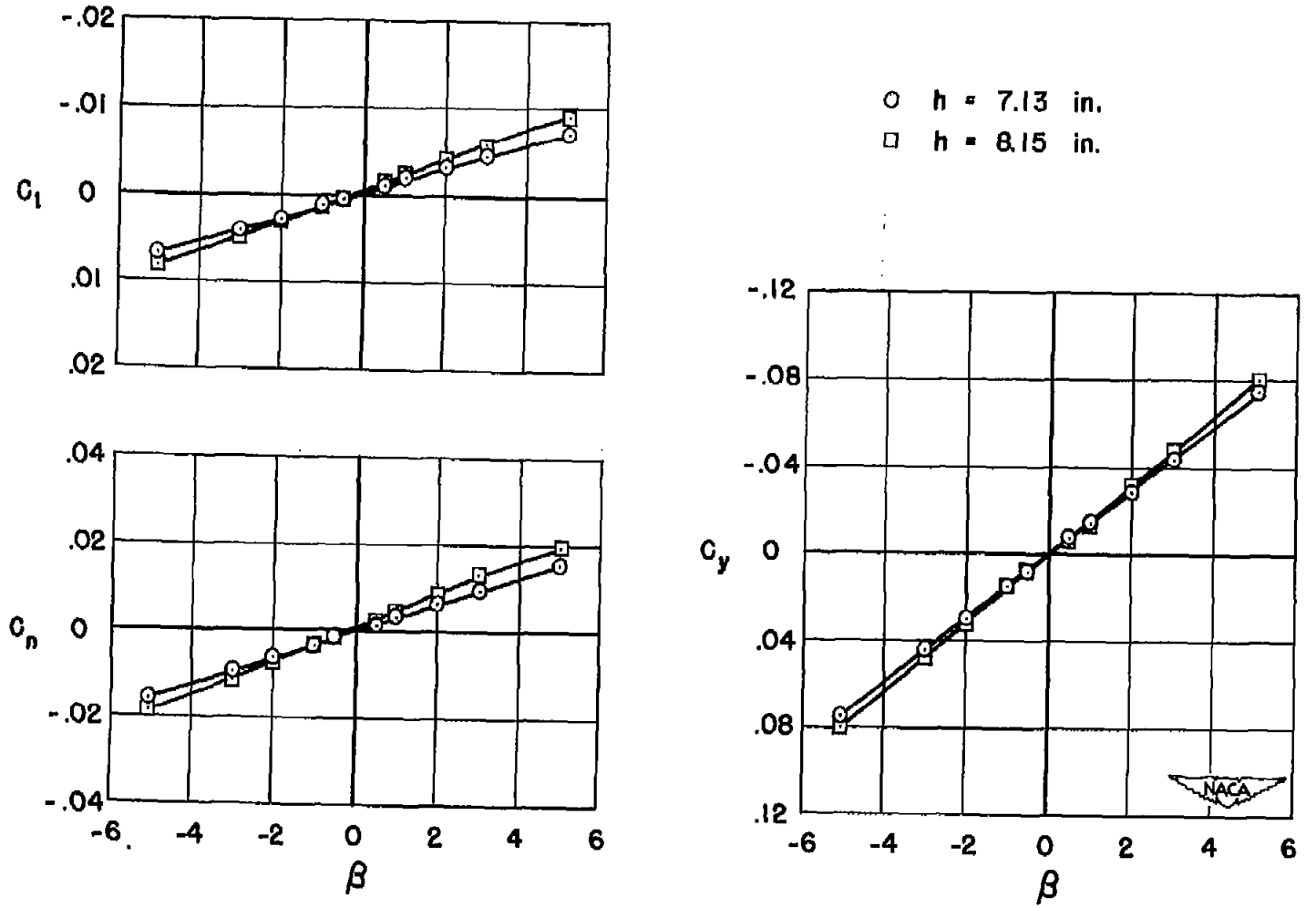

(c) M = 1.90

Figure 4.- Concluded.

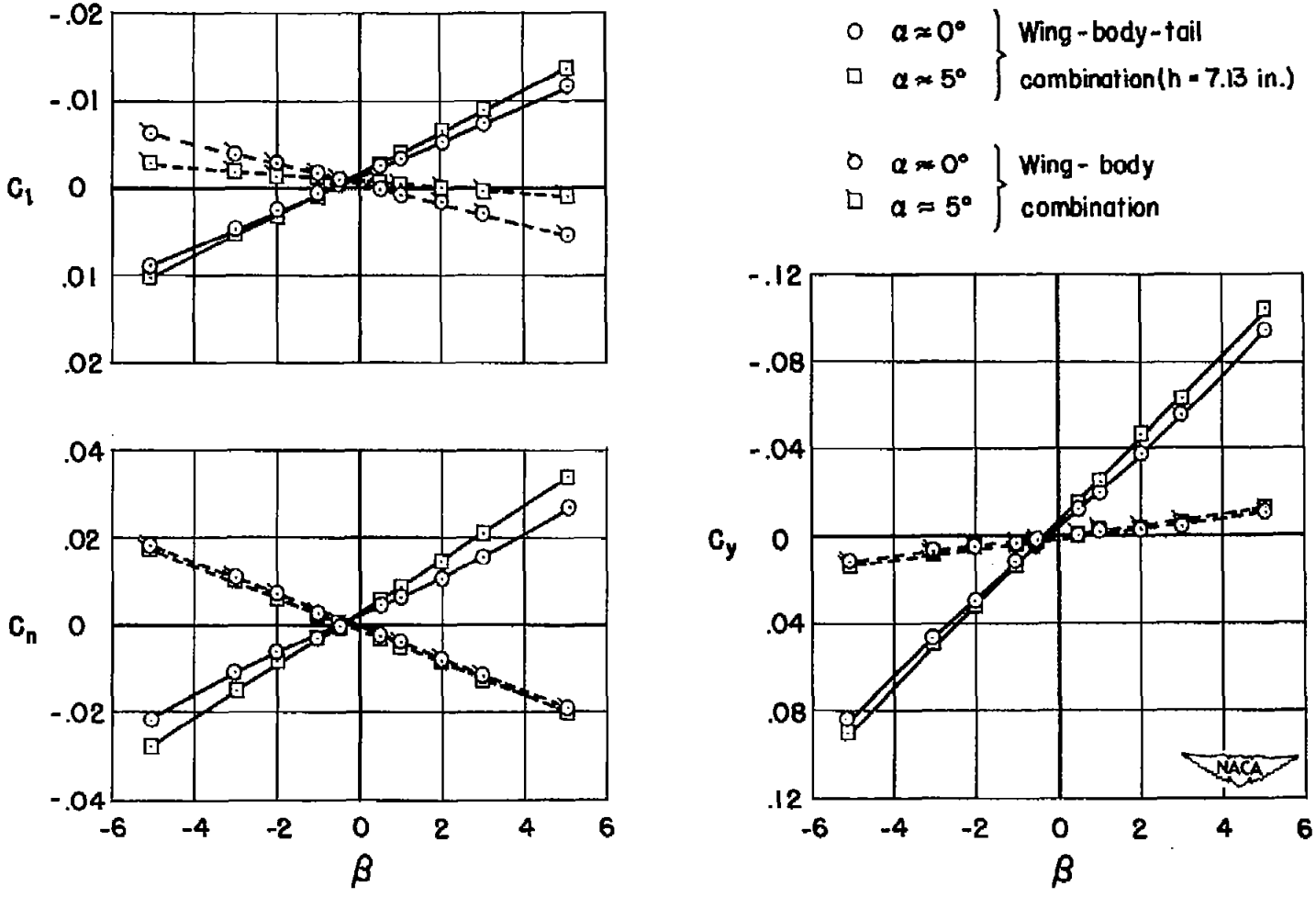

(a) M = 0.90

Figure 5.- Effect of angle of attack on the variation with sideslip angle of the rolling-moment, yawing moment, and cross-wind-force coefficients for a model of a fighter airplane; $\Gamma = -10^{\circ}$.

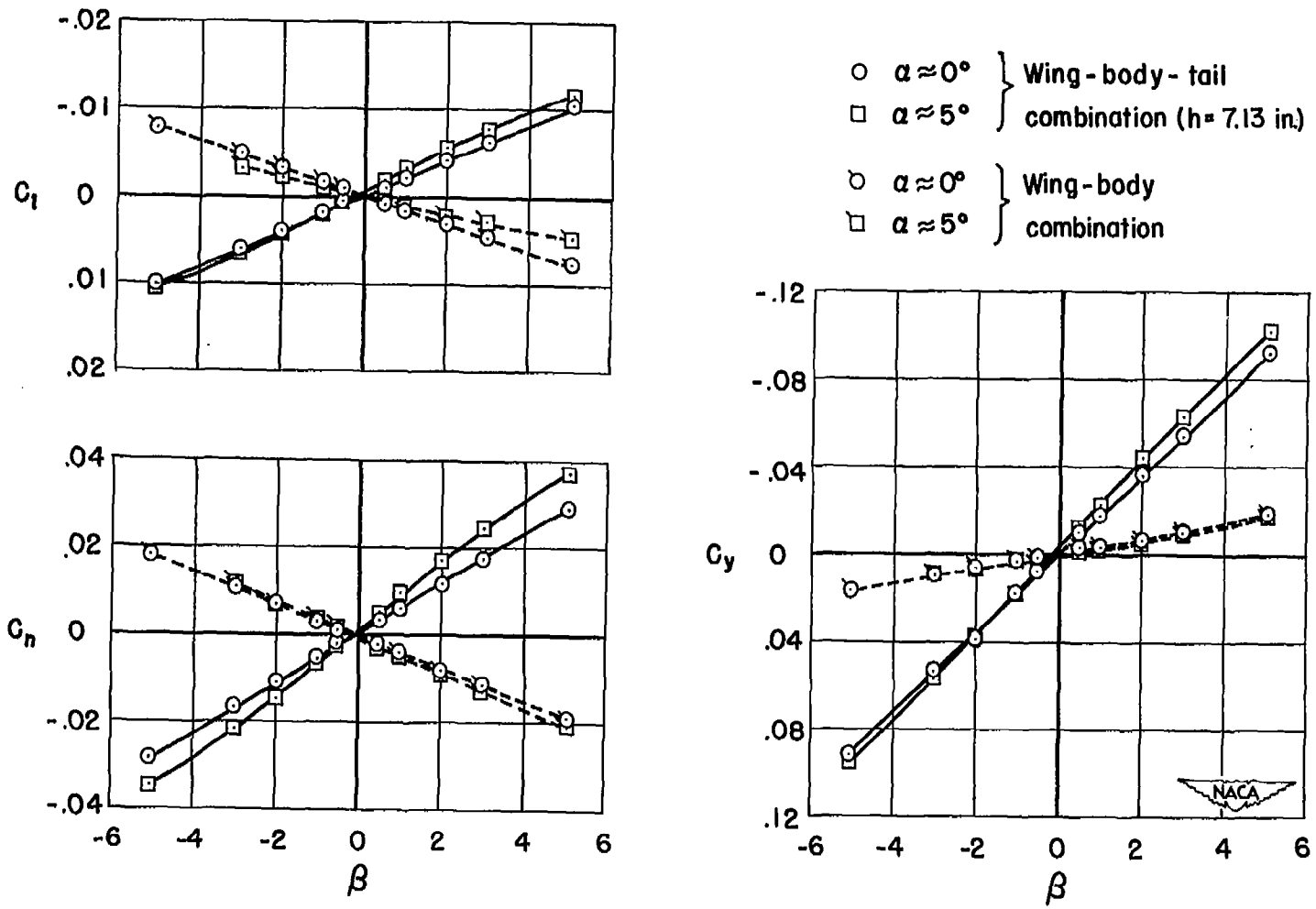

(b) M = 1.45

Figure 5.- Continued.

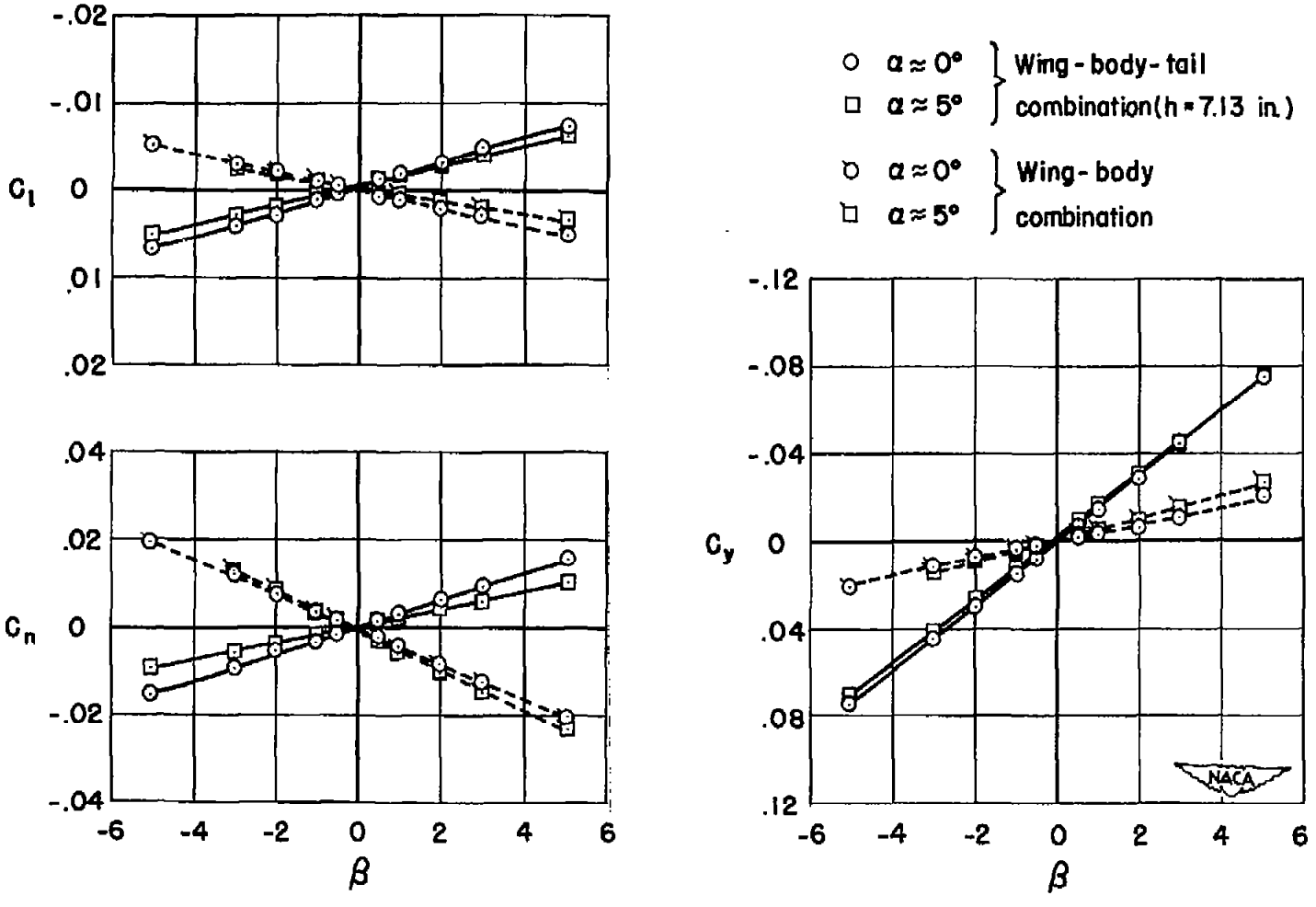

(c) M = 1.90

Figure 5.- Concluded.

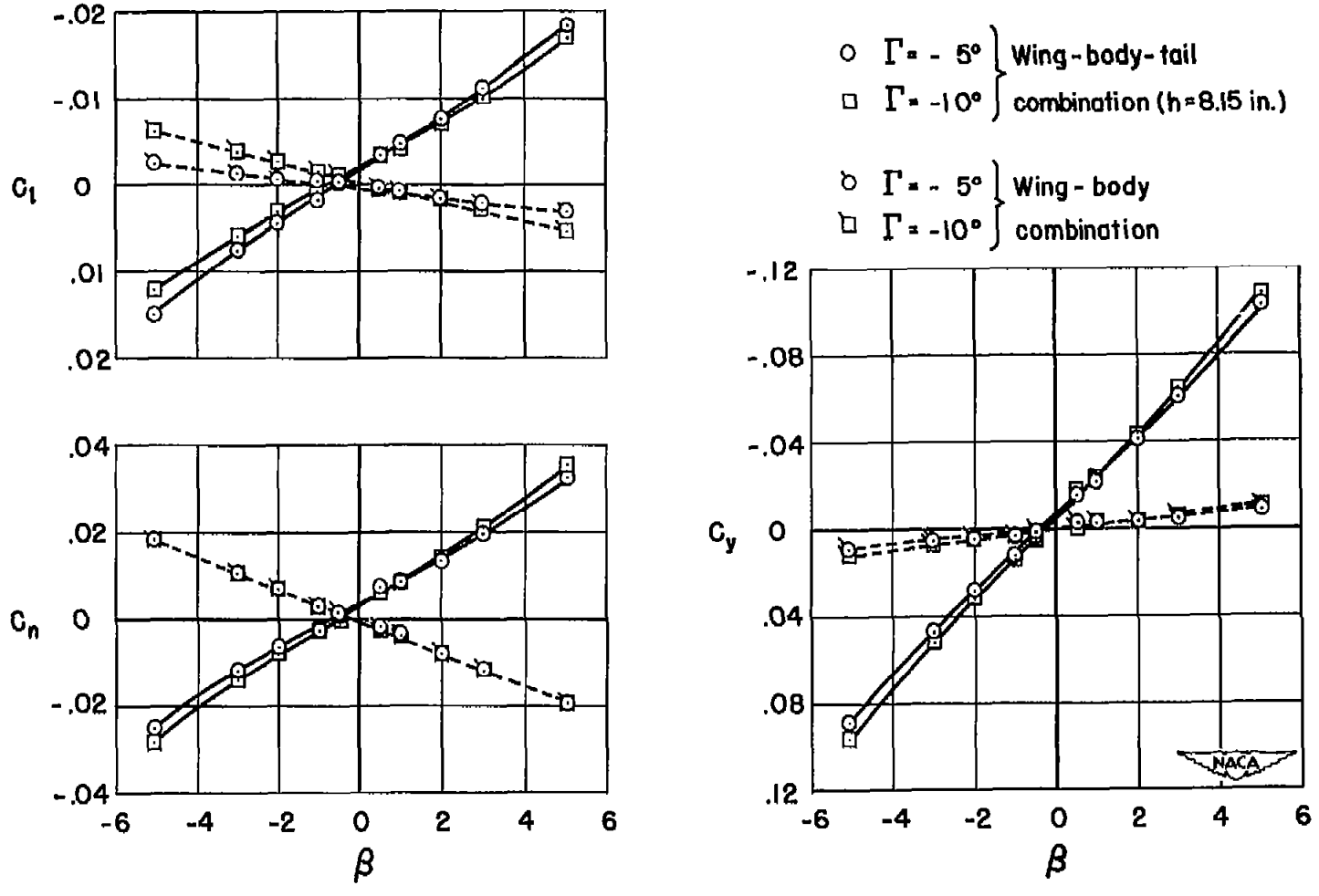

(a) M = 0.90

Figure 6.- Effect of wing dihedral on the variation with sideslip angle of the rolling-moment, yawing-moment, and cross-wind-force coefficients for a model of a fighter airplane; $\alpha \approx 0^{\circ}$.

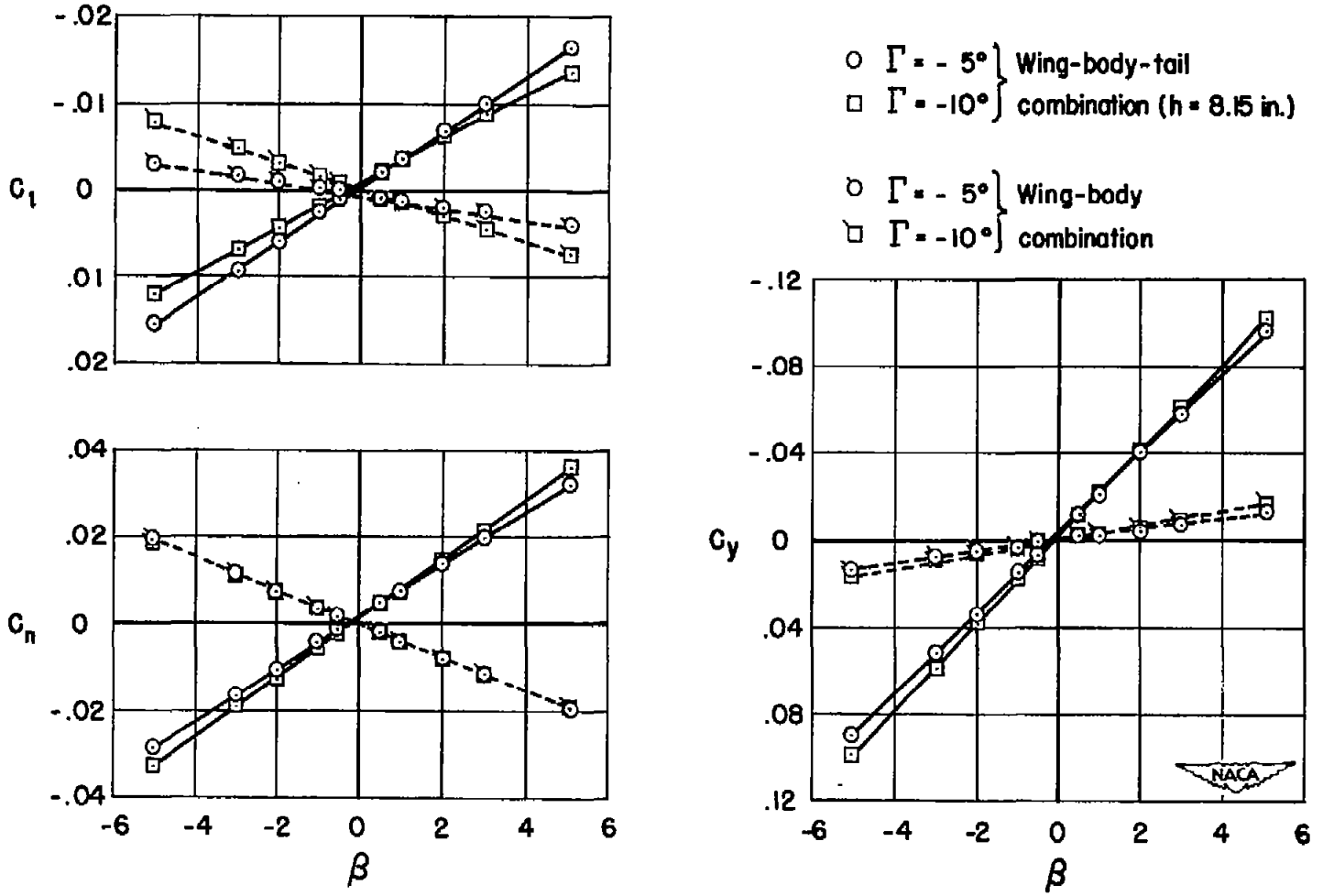

(b) M = 1.45

Figure 6.- Continued.

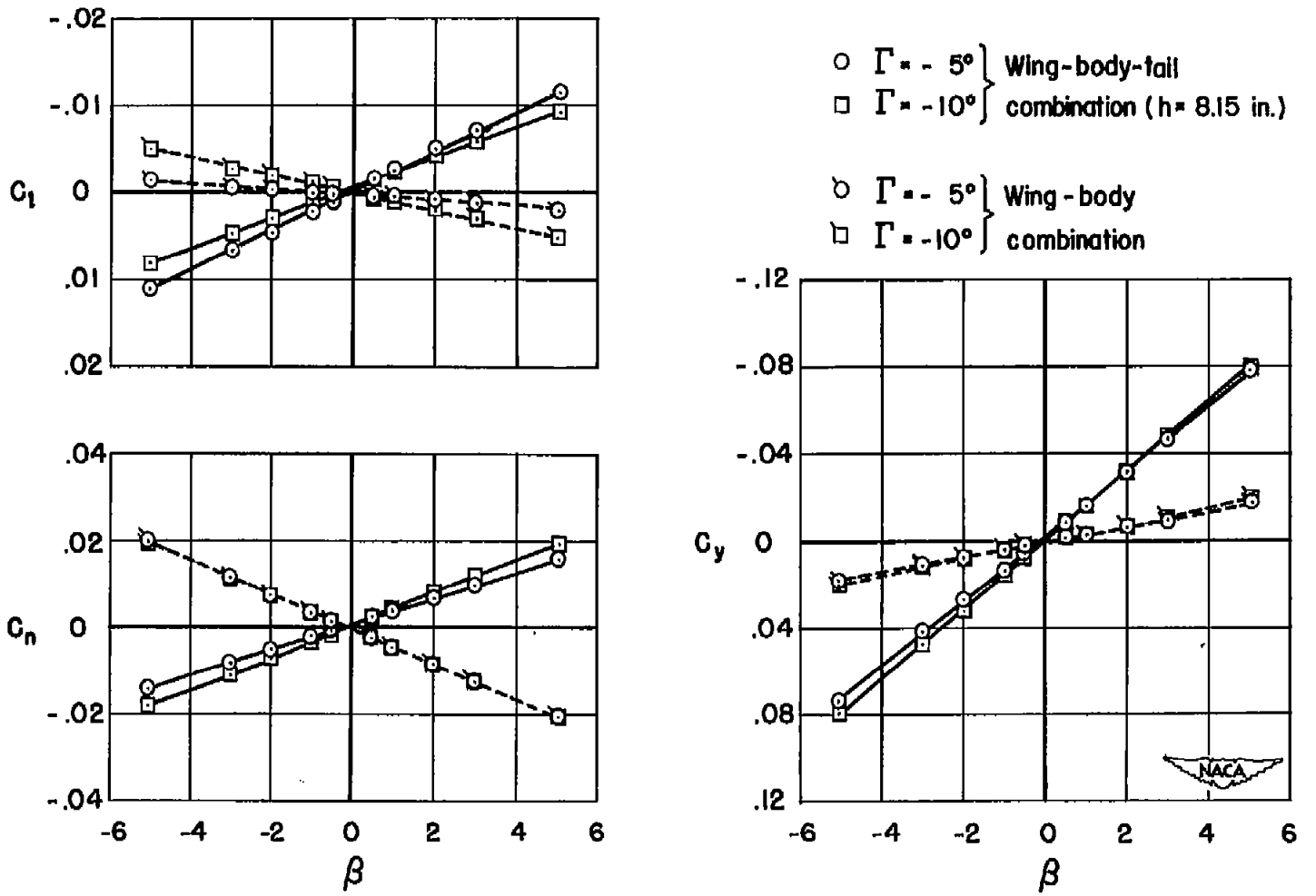

(c) M = 1.90

Figure 6.- Concluded.

DO NOT DETACH FROM REPORT
PLEASE LINE THROUGH YOUR NAME
BEFORE RETURNING TO THE LIBRARY

Name	Mail Stop
McMillin, N.	170